



**Effects of powder-to-liquid ratio on properties of  $\beta$ -tricalcium-phosphate cements modified using high-energy ball-milling**

Journal:	<i>Dental Materials Journal</i>
Manuscript ID	DMJ2016-341.R2
Manuscript Type:	Original paper
Date Submitted by the Author:	n/a
Complete List of Authors:	Ida, Yumika; Tokushima University Graduate School of Oral Science, Biomaterials and Bioengineering Bae, Jiyoung; Tokushima University Graduate School of Oral Science, Biomaterials and Bioengineering Sekine, Kazumitsu; Tokushima University; Tokushima University Graduate School of Oral Science Kawano, Fumiaki; Tokushima University Graduate School of Oral Science, Comprehensive Dentistry HAMADA, Kenichi; Tokushima University Graduate School of Oral Science, Biomaterials and Bioengineering
Keywords:	Injectability, $\beta$ -TCP, Mechanical properties, Compressive strength in vivo
Categories:	Bio-ceramics < Primary Research Field (Sub Field)

SCHOLARONE™  
Manuscripts

ORIGINAL PAPER

Effects of powder-to-liquid ratio on properties of  $\beta$ -tricalcium-phosphate cements modified using high-energy ball-milling

Yumika IDA<sup>a</sup>, Jiyoung BAE<sup>a</sup>, Kazumitsu SEKINE<sup>a</sup>, Fumiaki KAWANO<sup>b</sup>, Kenichi HAMADA<sup>a</sup>

<sup>a</sup>Department of Biomaterials and Bioengineering, Tokushima University Graduate School of Oral Science, 3-18-15 Kuramoto, Tokushima 770-8504, Japan.

<sup>b</sup>Department of Comprehensive Dentistry, Tokushima University Graduate School of Oral Science, 3-18-15 Kuramoto, Tokushima 770-8504, Japan.

Corresponding author: Jiyoung BAE

E-mail: [enchantee23@naver.com](mailto:enchantee23@naver.com)

Tel.: +81 88 633 7333

Fax: +81 88 633 9125

Keyword: Injectability,  $\beta$ -TCP, Mechanical properties, Compressive strength *in vivo*

Number of reprints: 50

**ABSTRACT**

The authors have developed a  $\beta$ -tricalcium-phosphate ( $\beta$ -TCP) powder modified mechano-chemically through the application of a ball-milling process (m $\beta$ -TCP). The resulting powder can be used in a calcium-phosphate-cement (CPC). In this study, the effects of the powder-to-liquid ratio (P/L ratio) on the properties of the CPCs were investigated, and an appropriate P/L ratio that would simultaneously improve injectability and strength was clarified. The m $\beta$ -TCP cement mixed at a P/L ratio of 2.5 and set in air exhibited sufficient injectability until 20 min after mixing, and strength similar to or higher than that mixed at a P/L ratio of 2.0 and 2.78. Although the m $\beta$ -TCP cements set *in vivo* and in SBF were found to exhibit a lower strength than those set in air, it did have an appropriate setting time and strength for clinical applications. In conclusion, P/L ratio optimization successfully improved the strength of injectable m $\beta$ -TCP cement.

## 1. Introduction

Calcium-phosphate-cements (CPCs) are widely used for bone repair and bone augmentation<sup>1-4)</sup>. However, one of the problems with currently available commercial CPCs is their poor injectability<sup>5, 6)</sup>. CPC pastes are required to exhibit a sufficient degree of injectability to enable minimally invasive bone-defect filling<sup>7)</sup>. A effective approach to improving the injectability is to reduce the powder-to-liquid ratio (P/L ratio) of the CPC<sup>8)</sup>. However, doing so adversely affects the mechanical properties of a CPC after setting, while simultaneously increasing the setting time<sup>3, 9)</sup>. An effective approach to improve the injectability is decreasing the particle size of CPC powder<sup>3)</sup>. One popular process to reduce the size is mechanical milling process. The authors have developed  $\beta$ -TCP powders, produced using a ball-milling process, as a new CPC constituent<sup>10)</sup>. A few previous researches evaluated the effects of mechanical milling of  $\beta$ -TCP powders on their properties, and they indicated significant improvement of CPC strength after setting using motor grinding<sup>11)</sup> and ball-milling<sup>12)</sup>. However, they did not evaluate the injectability of CPC paste. A CPC paste made of the modified  $\beta$ -TCP powders<sup>10)</sup> simultaneously exhibited better injectability and a shorter setting time than a paste made of conventional  $\beta$ -TCP powders with the same liquid and P/L ratio. Moreover, after setting, the CPC exhibited a higher strength. The modified  $\beta$ -TCP cement had an extremely high level of injectability, suggesting that the injectability would be sufficient despite the value falling as the P/L ratio increases. In addition, cements mixed with a higher P/L ratio should simultaneously exhibit a shorter setting time and higher strength<sup>3, 9, 13)</sup>.

There is no standard for evaluating injectability. However, a major parameter is the time that a CPC remains injectable from a syringe after mixing. Commercial CPCs remain injectable for a wide range of times, making it difficult to find an appropriate benchmark value. It has been suggested that a suitable injectable time is 12 min<sup>14)</sup>. In this study, the authors increased the P/L ratio to improve the setting time and strength while maintaining a sufficient degree of injectability until approximately 10 min after mixing. The calcium-to-phosphate molar ratio (Ca/P ratio) of the CPC after setting is also an important factor affecting the cement properties. In this study, the concentrations of  $\text{Ca}^{2+}$  and  $\text{PO}_4^{2-}$  in the liquid were adjusted to maintain a constant Ca/P ratio.

CPCs demonstrate self-setting both in SBF and *in vivo*; however, the properties of a CPC set in SBF differ from those of a CPC set *in vivo*. In particular, *in vivo* reported as being less complete<sup>15,16</sup>. Because a major clinical application of CPCs is the direct filling of bone defects, the CPC setting inevitably occurs *in vivo*. Hence, the properties of CPCs when set *in vivo* must be evaluated. The objective of this study was to investigate the effects of the P/L ratio on the properties of a CPC formulated using the modified  $\beta$ -TCP, and to clarify an appropriate P/L ratio to produce an injectable CPC paste. Moreover, the setting properties and strengths of cements set *in vivo* were investigated.

## 2. Materials and Methods

### 2.1. Preparation of $\beta$ -TCP and calcium-phosphate-cement

The CPC powder used in this study was a  $\beta$ -TCP powder (Taihei Chemical Industrial Co. Ltd., Osaka, Japan), as was used in a previous study<sup>10</sup>. The  $\beta$ -TCP powder was first crushed in a mortar and pestle and then further ground using an auto-mortar (ANM-200, Nitto Kagaku Co., Ltd., Nagoya, Japan), operating at 120 rpm for 30 min. The resulting  $\beta$ -TCP powder was evaluated as a control (control  $\beta$ -TCP; c $\beta$ -TCP) in this study. The median particle size and average crystal size of c $\beta$ -TCP was 2.5  $\mu\text{m}$  and 92 nm, respectively. The  $\beta$ -TCP powder was then milled using a planetary ball-mill (Pulverisette7, Fritsch GmbH, Idar-Oberstein, Germany). We placed 8 g of the  $\beta$ -TCP powder, 4  $\text{cm}^3$  of ethanol (99.5%), and seven zirconia balls (15 mm diameter, ditto) in a zirconia jar (45  $\text{cm}^3$ , ditto). The milling was performed at a rotational speed of approximately 1000 rpm, for working times of 1 h interspersed with intervals of 1 h, up to a total working time of 24 h. The resulting powder (modified  $\beta$ -TCP; m $\beta$ -TCP) was then dried in an oven at 60°C for 24 h. The median particle size and average crystal size of m $\beta$ -TCP was 1.6  $\mu\text{m}$  and 15 nm, respectively. To produce a CPC paste, the  $\beta$ -TCP powder was mixed with the two types of liquid listed in Table 1<sup>10,17</sup>. The P/L ratio of the m $\beta$ -TCP to the first liquid, a  $\text{CaCl}_2$  solution, and to the second liquid, a  $\text{NaH}_2\text{PO}_4$  solution, were 1 g:0.25  $\text{cm}^3$ :0.25  $\text{cm}^3$  (P/L: 2.0), 1 g:0.2  $\text{cm}^3$ :0.2  $\text{cm}^3$  (P/L: 2.5), and 1 g:0.18  $\text{cm}^3$ :0.18  $\text{cm}^3$  (P/L: 2.78), respectively. The  $\beta$ -TCP cements were mixed with  $\text{CaCl}_2$  solution first for 5 min and then with  $\text{NaH}_2\text{PO}_4$  solution for 1 min. The paste was manually mixed on a glass slab

using a stainless-steel spatula. The P/L ratio of the  $\alpha$ -TCP powder was 2.0, and the Ca/P ratio of the liquid used in this study was 1.67.

## 2.2. Injectability evaluation

To evaluate the injectability, 5.5 g of  $\beta$ -TCP cement paste was placed in a disposable syringe (Terumo Syringe, Terumo Corp., Tokyo, Japan) immediately after mixing. The syringe had an opening with a 2-mm inner diameter, a body with a 13-mm inner diameter, and a total internal volume of 6 mm<sup>3</sup>. After being filled with  $\beta$ -TCP cement, each syringe was stored in an incubator at 37°C and a humidity of 100%. Then, the cement was allowed to set. The plunger of the syringe was loaded using a universal test machine (frame: Auto-graph AGS-500A; load cell: Type SLBL-1kN, Shimadzu Corp., Kyoto, Japan) at a constant cross-head speed of 20 mm/min until the load reached 300 N. The mass of the  $\beta$ -TCP cement paste ejected from the syringe was measured and the injectability was calculated as:

$$I = M_i/M_0 \quad (1)$$

where  $I$  is the injectability,  $M_i$  is the mass of cement paste ejected, and  $M_0$  is the initial mass of cement paste in the syringe.

## 2.3. Mechanical property evaluation

The compressive strength (CS) and diametral tensile strength (DTS) of the  $\beta$ -TCP cements were evaluated. The specimens prepared for CS evaluation were 3 mm in diameter and 6 mm in height, while those for DTS evaluation were 6 mm in diameter and 4 mm in height. These were produced using molds formed from silicone rubber (KE-1300T, Shin-Etsu Chemical Co., Ltd., Tokyo, Japan). Cement paste was placed in the molds using a stainless steel spatula, and pushed into the corners of the mold using a toothpick to eliminate any large voids. The specimens were then placed in an incubator at 37°C and a humidity of 100% to set for 1 h to 5 h, 1 day, 3 days, 1 week, and 2 weeks. After setting, the specimens were carefully extracted from the mold, and then dried in air at 60°C for 24 h. The dimensions of the specimens after

drying were measured using a digital caliper. The crosshead speed used for CS and DTS evaluation was 10 mm/min, that is, the strain rate for the CS and DTS evaluation was  $1.0 \times 10^{-2}$ /s and  $6.6 \times 10^{-3}$ /s, respectively. Twenty specimens were prepared for testing under each condition.

#### 2.4. Porosity evaluation

The density and porosity of the  $\beta$ -TCP cement were measured using the DTS evaluation specimens after being in the incubator for 1 week. Three specimens were evaluated for each P/L ratio. The weight of each specimen was measured using a microbalance, and the apparent density was calculated from the weight and the specimen volume. The real density was measured three times for each specimen using a gas pycnometer (AccuPyc 1330, Micromeritics Instrument Inc., Norcross, GA, USA). The porosity of the specimen was calculated as:

$$P (\%) = (1 - \rho_a/\rho_r) \times 100 \quad (2)$$

where  $P$  is the porosity,  $\rho_a$  is the apparent density, and  $\rho_r$  is the real density.

#### 2.5. Microstructure observation

The fracture surface of the DTS evaluation specimens, 2 weeks after mixing, were gold-coated using an ion-coater (IB-3, Eiko Engineering Co. Ltd., Tokyo, Japan), and then observed using a scanning electron microscope (SEM; JCM5700, JEOL Ltd., Tokyo, Japan).

#### 2.6. Evaluation of crystallization and degradation *in vivo* and in simulated body fluid

The crystallization and degradation of the  $\beta$ -TCP cement *in vivo* were evaluated. We purchased six male 5-week-old Sprague-Dawley rats (CLEA Japan Inc., Tokyo, Japan), and fed them for 1 week following the fundamental guidelines for the proper conduct of animal experiments under Japanese law, and with the approval of the Tokushima University animal administration. Upon reaching 5 weeks, all of the rats, which had an initial weight of

311.7±9.8 g were anesthetized using a weight-adjusted peritoneal injection of pentobarbital sodium salt (45 mg/kg). Under anesthesia, each rat's back skin was shaved, and then cleaned with Betadine (Meiji Seika Pharma, Tokyo, Japan). Two incisions of around 50 mm in length were made in the left and right sides of the shaved parts. To insert the cement specimens, three pockets were formed in the subcutaneous fascia and the skin on each side of the rats' backs. The  $\beta$ -TCP cement specimens were prepared while the surgery was ongoing, and were immediately placed in the pocket. The  $\beta$ -TCP cement powder and the tools used for mixing the cement were sterilized by ethylene oxide, and the liquid components were sterilized using a 0.45- $\mu$ m mesh syringe filter. The mixed  $\beta$ -TCP cement paste was filled into a molds made of silicone rubber (KE-1300T, Shin-Etsu Chemical Co., Ltd., Tokyo, Japan). These molds were 6 mm high, with an outer diameter of 6 mm and an inner diameter of 3 mm. We allowed 5 min to elapse after placing the paste into the molds, then three of the c $\beta$ -TCP cement specimens, still in their molds, were inserted into the left pockets, and three m $\beta$ -TCP (P/L: 2.5) cement specimens, again in their molds, were installed into the right pockets. We were obliged to insert the samples complete with the mold because, 5 min after filling, the cement samples did not appear to be strong enough to be extracted from the mold. After specimen insertion, each pocket was closed using Vicryl needles (Johnson & Johnson Co., Ltd., Tokyo, Japan), and the fascia and skin were sutured. The rats were sacrificed by an over-administration of pentobarbital sodium salt, 1 week, 2 weeks, and 4 weeks after the insertion of the samples. The cement specimens, still in their molds, were removed carefully, and then dried in a convection oven at 60°C for 1 h. Then, the specimens were gently extracted from their molds. The dimensions of those specimens exhibiting sufficient toughness were measured using a digital caliper, and then a CS evaluation was performed. After the CS evaluation, the fractured specimen was ground into a fine powder, and the phase constitution was analyzed using X-ray diffractometry (XRD) with a Cu K $\alpha$  source at 30 kV and 15 mA.

To clarify the effect of the cement setting conditions on the crystallization of hydroxyapatite (HAp),  $\beta$ -TCP cement which had been set in a simulated body fluid (SBF , ISO23317: 2014) was also evaluated. Specimens of c $\beta$ -TCP cement and m $\beta$ -TCP (2.5) cement with the same dimensions as the CS mold were prepared. After placing the cement paste in

the molds, we allowed 5 min to elapse and then placed three of the cement specimens in 30 cm<sup>3</sup> SBF in a 160-cm<sup>3</sup> Teflon bottle for 1 week, 2 weeks, and 4 weeks in an incubator at 37°C. After soaking, a CS evaluation and XRD analysis were performed using the same procedures as those used to examine the samples inserted into the rats.

## 2.7. Statistical evaluation

All of the data were statistically analyzed by Steel-Dwass Test using EZR software (Saitama Medical Center, Jichi Medical University, Japan)<sup>18)</sup> to compare the means of the different groups. The statistical significance was accepted at the 0.05 (number of specimen, n = 5 or 6) or 0.01 (n = 20) confidence level.

## 3. Results

### 3.1. Injectability of $\beta$ -TCP cement paste

Figure 1 shows the injectability of the  $\beta$ -TCP cement paste. The injectability was found to decrease as the P/L ratio increased. The paste of m $\beta$ -TCP (2.78) cement was not injectable 5 min after mixing, while that of m $\beta$ -TCP (2.5) cement could be injected up until 20 min after mixing. Solid-liquid phase separation during injection was not observed in each paste.

### 3.2. Mechanical properties of $\beta$ -TCP specimen

Figures 2 and 3 show the initial CS and DTS up until 5 h after mixing. The CS and DTS of the c $\beta$ -TCP cement specimens 5 h after mixing were 1.0±0.4 MPa and near zero, respectively. The initial strength of the m $\beta$ -TCP cement specimens increased with the P/L ratio. The CS and DTS values of the m $\beta$ -TCP (2.0) cement samples increased from 3 h to 4 h and from 2 h to 3 h after mixing, respectively. The CS values of the m $\beta$ -TCP (2.78) cement specimens up until 3 h after mixing were higher than those of the m $\beta$ -TCP (2.5) cement specimens. However, 4 h and 5 h after mixing, the two cement specimens exhibited similar strengths. The DTS values of the m $\beta$ -TCP (2.78) cement specimens exhibited values that were lower than or similar to those of the m $\beta$ -TCP (2.5) cement specimens. Figure 4 shows the change in the CS of the c $\beta$ -TCP and m $\beta$ -TCP specimens with time after mixing. Although the mean value of the

CS of the m $\beta$ -TCP (2.0) cement samples exhibited a slow increase from 1 day to 2 weeks, there was no significant difference. The CS of the m $\beta$ -TCP (2.5 and 2.78) cement specimens 3 days after mixing was higher than that at 1 day. However, there were no significant changes between 3 days and 2 weeks after mixing. Figure 5 shows the DTS of the c $\beta$ -TCP and m $\beta$ -TCP specimens according to the time after mixing. The mean DTS value for the m $\beta$ -TCP (2.0 and 2.5) cement specimens exhibited a gradual increase from 3 days to 2 weeks. The DTS of the m $\beta$ -TCP (2.78) cement specimens were not significantly different from those of the m $\beta$ -TCP (2.5) cement specimens.

### 3.3. SEM observations of $\beta$ -TCP cement specimens

Figure 6 shows the fracture surfaces of the DTS specimen of the  $\beta$ -TCP cement specimen, 2 weeks after mixing. It was possible to observe long needle-like crystals and many pores in the granule structure on the fracture surface of the c $\beta$ -TCP cement specimens. On the fracture surfaces of the m $\beta$ -TCP (2.0) cement specimens, agglomerated plate-like crystals could be observed as indicated by the black arrows in Figure 6, and the number and size of the pores in the granule structure was smaller than those in the c $\beta$ -TCP cement specimen were. On the fracture surface of the m $\beta$ -TCP (2.5) cement specimen, the growth of numerous agglomerate grains was observed, and the crystal growth among the agglomerate grains was more distinct than that of the m $\beta$ -TCP (2.0) cement specimen. Conversely, the fracture surface of the m $\beta$ -TCP (2.78) cement specimen exhibited more and larger pores among the agglomerate grains compared with those of the m $\beta$ -TCP (2.5) cement specimens (as indicated by the arrow in Figure 6).

### 3.4. Porosity of $\beta$ -TCP cement specimen

Table 2 lists the porosities of the m $\beta$ -TCP specimens 1 week after mixing, according to the P/L ratio. The m $\beta$ -TCP (2.5) specimens, 1 week after mixing, exhibited the lowest porosity while the m $\beta$ -TCP (2.78) specimens, 1 week after mixing, exhibited the highest porosity.

### 3.5. Crystallization and degradation of $\beta$ -TCP cement specimens *in vivo*

The typical appearance of the cement specimens, 2 weeks after implantation in the backs of the rats, is shown in Figure 7. Many connective adhesions were observed between the c $\beta$ -TCP cement specimen and muscle fascia, and the surfaces of some the c $\beta$ -TCP specimens were peeled off and bonded to the muscle fascia (as indicated by the arrow in Figure 7). Therefore, the shapes of some of the c $\beta$ -TCP specimens after being extracted from their molds differed from those used for CS evaluation, resulting in the number of c $\beta$ -TCP specimens for CS evaluation being less than that of the m $\beta$ -TCP specimens. In contrast, few of the m $\beta$ -TCP specimens exhibited a change in shape after being extracted from their molds, because there were very few connective adhesions, and therefore little damage to the specimen. The condition of the specimens extracted from the molds, 1 week and 4 weeks after being inserted, was similar.

Figure 8 shows the CS test results for the  $\beta$ -TCP specimens set in SBF and *in vivo*. The c $\beta$ -TCP specimens set *in vivo* produced CS values similar to those of the c $\beta$ -TCP specimens set in air, as shown in Figure 4. The CS values of the c $\beta$ -TCP specimens set for 4 weeks *in vivo* were not evaluated, because the shape of the specimens after retrieval was not appropriate for testing. The m $\beta$ -TCP specimens set *in vivo* produced higher CS values than those of the c $\beta$ -TCP specimens, specifically, 17.9 MPa after being implanted for 2 weeks. The m $\beta$ -TCP specimens set in SBF also showed higher CS values than those of the c $\beta$ -TCP specimens, that is, 26.1 MPa after soaking for 2 weeks. Because of the large deviation in the CS values, the CS values of the m $\beta$ -TCP specimens set in SBF and *in vivo* were not significantly different after each implantation or soaking period, resulting in the implantation period having no significant effect on the CS values of the m $\beta$ -TCP specimens set *in vivo*. Meanwhile, there was a significant difference between the CS values of the m $\beta$ -TCP specimens set in SBF for 1 week and 2 weeks.

Figure 9 shows the XRD profiles of the m $\beta$ -TCP cement specimens set in SBF and *in vivo* for 1 week, 2 weeks, and 4 weeks, and those of the cement specimens set in air for 1 week. We can see HAp peaks in each profile, indicating that large amounts of HAp precipitates formed regardless of the setting conditions. We can also see  $\beta$ -TCP peaks in each profile of the m $\beta$ -TCP cement specimens set *in vivo*, and set in SBF. However,  $\beta$ -TCP peaks

in profile of the specimens set in SBF were broader and smaller than those set *in vivo*. While  $\beta$ -TCP peaks could not be observed in those of  $m\beta$ -TCP cement specimens set in air. These results suggest that most of the  $\beta$ -TCP in the  $m\beta$ -TCP cement paste set in SBF and that in the control cement paste, dissolved and was converted to HAp precipitate. However, the  $\beta$ -TCP in the  $m\beta$ -TCP cement paste set *in vivo* partially dissolved, with the  $\beta$ -TCP crystals remaining the cement specimen.

## 4. Discussion

### 4.1. Injectability of $\beta$ -TCP cement paste

The injectability of CPC is generally evaluated by ejecting a mass of CPC paste from a syringe subjected to a load. However, there are no standard test conditions governing the loading force, loading speed, size of syringe, and size of opening. Therefore, it is difficult to make comparisons with the values obtained for injectability in other studies. The  $m\beta$ -TCP (2.5) remained injectable for more than 20 min, much longer than the generally required value of 12 min<sup>14</sup>). Moreover, it is not clear that the injectability of  $m\beta$ -TCP (2.5) 10 min after mixing, approximately 20% was sufficient. However, these values can be optimized by changing the test conditions. Therefore, the injectability of  $m\beta$ -TCP (2.5) would appear to be well-suited to clinical applications.

### 4.2. Strength of $\beta$ -TCP specimens

The initial CS values of the  $m\beta$ -TCP (2.0) and  $m\beta$ -TCP (2.5) specimens exhibited a steep increase between 3 h and 4 h after mixing, while the initial CS values of the  $m\beta$ -TCP (2.78) did not exhibit such an increase between 1 h and 5 h after mixing. The steep increase in the CS values pointed to the rapid growth of the HAp crystals during the period, with the rapid HAp crystal growth of the CS of the  $m\beta$ -TCP (2.78) specimens starting within 1 h of mixing. The initial DTS values of the  $m\beta$ -TCP (2.0) specimen exhibited a steep increase between 2 h and 3 h after mixing, while those of the  $m\beta$ -TCP (2.5) and  $m\beta$ -TCP (2.78) specimens did not exhibit such an increase between 1 h and 5 h after mixing. The steep increase in the DTS values also suggests the rapid growth of the HAp crystals during this period. However, there

were some differences between the dependence of the CS and DTS values on time after mixing, as well as in the P/L ratio. One difference was that the period in which the steep increase occurred was not consistent, while another was that the CS value increased or saturated with the P/L ratio while some DTS values of the m $\beta$ -TCP (2.78) specimens were smaller than those of the m $\beta$ -TCP (2.5) specimens. The dominant factors affecting the CS and DTS values of brittle materials are different; the tensile strength is sensitive to the maximum size of defects in the specimen, while the compressive strength is not. With the progress of HAp crystal growth, the defects in the specimen, mainly pores in this study, possibly decreased in number and size, while the CS and DTS values simultaneously increased. However, the effect of reducing the number and size of the defects on the CS value was different from that on the DTS value, resulting in the difference in the duration of the steep increase. Although porosity data was not obtained for the specimens during the initial setting, the fracture surfaces of the CPC after the DTS test, as shown in Fig. 6, suggested that relatively larger pores could be observed in the m $\beta$ -TCP (2.0) and m $\beta$ -TCP (2.78) specimens. However, the size of the pores observed in the m $\beta$ -TCP (2.5) specimens was smaller. This smaller maximum pore size was one possible reason for the larger DTS of the m $\beta$ -TCP (2.5) specimens.

Because it was difficult to mix the m $\beta$ -TCP (2.78) paste, therefore limiting the time available for handling, there was not sufficient time to force the CPC paste into the corners of the molds. This insufficient filling of the CPC paste led to there being pores in the CS specimen that were so large that it is likely that the HAp crystals could not fill them. This is one possible reason for the CS values for m $\beta$ -TCP (2.78) being lower than those for m $\beta$ -TCP (2.5) from 1 day to 2 weeks after CPC mixing. In contrast, because the DTS specimen is larger than the CS specimen, it was not difficult to force the CPC paste into the corners of the molds. It suggested that the pore sizes in the m $\beta$ -TCP (2.78) DTS specimens were smaller than those in the CS specimens. This is one reason for the DTS values of m $\beta$ -TCP (2.78) being similar to those of m $\beta$ -TCP (2.5).

Figure 10 shows the correlation between the DTS and porosity of the m $\beta$ -TCP specimens 1 week after mixing. The m $\beta$ -TCP (2.5) appears to have a lower porosity than the

m $\beta$ -TCP (2.0), resulting in a higher DTS value than the m $\beta$ -TCP (2.0). Meanwhile, the m $\beta$ -TCP (2.78) had a higher porosity than the m $\beta$ -TCP (2.5), resulting in the lower DTS value than that of m $\beta$ -TCP (2.5). However, the increase in the DTS value from m $\beta$ -TCP (2.0) to m $\beta$ -TCP (2.78) with the porosity indicated that the porosity is not the only dominant factor affecting the DTS value. Another potential factor is the density of the HAp precipitations. Because the dense HAp precipitations in the agglomerate grains of the CPC specimen possibly contribute to the high strength of the grain, the DTS value of a CPC specimen with a high P/L ratio could be higher. The above two factors simultaneously affected the DTS value of the m $\beta$ -TCP (2.78) cement in this study, resulting in a DTS value higher than that of the m $\beta$ -TCP (2.0) but lower than that of the m $\beta$ -TCP (2.5).

#### **4.3. Microstructure of $\beta$ -TCP specimen**

The precipitated needle-like HAp crystals of c $\beta$ -TCP cement did not form a network, resulting in the low strength of the c $\beta$ -TCP. As the P/L ratio increased, the granular structure became very difficult to observe, and a dense HAp precipitation network was formed. This dense network gives rise to a higher strength and faster setting.

#### **4.4. Crystallization and degradation of $\beta$ -TCP cement specimens *in vivo***

In this study,  $\beta$ -TCP cement specimens, still in their molds, were inserted into pockets formed in the backs of rats. The molds were used to maintain the shape of the specimen while the cement was setting. This procedure was required for CS evaluation; however, the specimens differed from the CPC injected into bone defects. The side surfaces of the cylindrical specimens were covered by the mold and therefore were not in direct contact with their surroundings, that is, hard and/or soft tissue, and body fluids. Therefore, the effects of the *in vivo* setting of the cement as observed in this study were quantitatively limited. However, they could suggest a qualitative effect.

Only the c $\beta$ -TCP specimens proved difficult to retrieve without damage, due to the formation of connective tissue between the muscle fascia and the specimen. A major reason for this was the slow setting of the c $\beta$ -TCP cement; the slow growth of the HAp precipitates

allowed the growth of connective tissue into the specimen. Another major reason was the large number and size of the pores in the specimen; the space enhanced body fluid flow into the specimen, and thus supported the growth of connective tissue. With the increase in the time after cement mixing, both the growth of the HAp precipitates and that of the connective tissue progressed, thus enhancing the interaction between them. This was one possible reason why the damage to the specimen retrieved after being implanted for 4 weeks was conspicuous, such that CS evaluation could not be performed.

The CS value of m $\beta$ -TCP cement set in SBF and that set *in vivo* were significantly smaller than that set in air. One potential reason for this is the reduction in the liquid concentration; because the cement paste is in direct contact with the SBF or body fluid, Ca<sup>2+</sup> and PO<sub>4</sub><sup>2-</sup> in the liquid could diffuse into the surrounding liquid. The Ca<sup>2+</sup> and PO<sub>4</sub><sup>2-</sup> concentrations in the cement paste were difficult to evaluate. However, it was high enough to precipitate HAp. In contrast, the concentrations of SBF and body fluid are not sufficient to precipitate HAp. Therefore, the concentrations of the cement paste are potentially higher than those of the SBF and body fluid. Thus, the Ca<sup>2+</sup> and PO<sub>4</sub><sup>2-</sup> in the cement paste will diffuse into the SBF or body fluid, resulting in the reduction of the Ca<sup>2+</sup> and PO<sub>4</sub><sup>2-</sup> concentrations of the cement paste. This reduction suppressed HAp precipitation, and either reduced the CS value of the cement or delayed the CS increase.

Another reason for the m $\beta$ -TCP cement set *in vivo* having lower CS than that set in air was the body fluid contamination of the cement paste. Blood contamination of the liquid in the cement has been reported to reduce the strength of a cement specimen<sup>16)</sup>. In this study, the source of the contamination was not blood, but the organic content of the body fluids could reduce the strength of the cement in a similar manner. Therefore, the cement could deform as it was setting, thus damaging the HAp crystal precipitates, and suppressing the growth of the HAp crystal network. Nevertheless, there was no significant difference between the CS value of cement set *in vivo* and in SBF 4 weeks after mixing. Therefore, the above mechanism whereby the CS value of a cement specimen is reduced did not have a significant effect in this study. A potential reason for this diminished effect on the CS value of a cement specimen was the quick setting *in vivo* and in SBF.

On the other hand, it is possible to observe a difference in the increase in the CS value according to the time that has elapsed since mixing. Although there was no significant difference between the CS value of m $\beta$ -TCP cement set *in vivo*, the average value increased according to the time after mixing. In contrast, the CS value of the m $\beta$ -TCP cement set in SBF increased up until 2 weeks after mixing and then exhibited saturation, while that of the m $\beta$ -TCP cement set in air increased until 3 days after mixing, at which point it exhibited saturation. These results suggest that the time at which the CS value reaches saturation increases in the order of setting in air, setting in SBF, and setting *in vivo*. This order suggests the order in which the setting of the cement is delayed. However, the setting time of the m $\beta$ -TCP cement *in vivo* was much shorter than that of the c $\beta$ -TCP cement, and is responsible for the washing-out of the cement *in vivo*. This is the main clinical advantage of the m $\beta$ -TCP cement developed as part of this research.

## 5. Conclusions

In a previous study, m $\beta$ -TCP (2.0) cement exhibited excellent injectability even 1 h after mixing. Therefore, the P/L ratio of  $\beta$ -TCP cement can be reduced to increase the strength of the cement while maintaining a sufficient degree of injectability. The m $\beta$ -TCP (2.5) cement paste remained sufficiently injectable up until 20 min after mixing. The initial CS and DTS values of the m $\beta$ -TCP (2.5) cement specimens, set in air, 4 h and 5 h after mixing were similar to or higher than those of m $\beta$ -TCP (2.78). The maximum CS and DTS values of the m $\beta$ -TCP (2.5) cement specimens set in air were 44.6 MPa and 7.4 MPa, respectively. These values were similar to those of m $\beta$ -TCP (2.78). The CS values of m $\beta$ -TCP (2.5) cement set in SBF and *in vivo* were significantly smaller than those of the specimens set in air. However, the values obtained demonstrated that the m $\beta$ -TCP cement used in this study is a promising candidate for application to many clinical scenarios.

## Acknowledgment

This work was partially supported by the Japan Society for the Promotion of Science (JSPS. KAKENHI Grant number 16K20504 and 16K11626).

## References

- 1) Bohner M, Gbureck U, Barralet J. Technological issues for the development of more efficient calcium phosphate bone cements: a critical assessment. *Biomaterials* 2005; 26: 6423-9.
- 2) Dorozhkin SV. Bioceramics of calcium orthophosphates. *Biomaterials* 2010; 31: 1465-85.
- 3) Dorozhkin SV. Self-Setting Calcium Orthophosphate Formulations. *Journal of Functional Biomaterials* 2013; 4: 209-311.
- 4) Zhang J, Liu W, Schnitzler V, Tancret F, Bouler J-M. Calcium phosphate cements for bone substitution: Chemistry, handling and mechanical properties. *Acta biomaterialia* 2014; 10: 1035-49.
- 5) Baroud G, Cayer E, Bohner M. Rheological characterization of concentrated aqueous  $\beta$ -tricalcium phosphate suspensions: The effect of liquid-to-powder ratio, milling time, and additives. *Acta biomaterialia* 2005; 1: 357-63.
- 6) Bohner M, Baroud G. Injectability of calcium phosphate pastes. *Biomaterials* 2005; 26: 1553-63.
- 7) Alshaaer M, Kailani MH, Jafar H, Ababneh N, Awidi A. Physicochemical and Microstructural Characterization of Injectable Load-Bearing Calcium Phosphate Scaffold. *Advances in Materials Science and Engineering* 2013; 2013.
- 8) Gbureck U, Barralet JE, Spatz K, Grover LM, Thull R. Ionic modification of calcium phosphate cement viscosity. Part I: hypodermic injection and strength improvement of apatite cement. *Biomaterials* 2004; 25: 2187-95.
- 9) Barralet J, Grover L, Gbureck U. Ionic modification of calcium phosphate cement viscosity. Part II: hypodermic injection and strength improvement of brushite cement. *Biomaterials* 2004; 25: 2197-203.
- 10) Bae J, Ida Y, Sekine K, Kawano F, Hamada K. Effects of high-energy ball-milling on injectability and strength of  $\beta$ -tricalcium-phosphate cement. *Journal of the mechanical behavior of biomedical materials* 2015; 47: 77-86.

- 11) Sakamoto K, Hoshina K, Yamaguchi S, Fujihara I, Satoh K, Tsunawaki Y. HARDENING OF BETA.-TRICALCIUM PHOSPHATE MECHANICALLY TREATED BY MORTAR GRINDER. *Phosphorus Research Bulletin* 2011; 25: 64-7.
- 12) Gbureck U, Grolms O, Barralet J, Grover L, Thull R. Mechanical activation and cement formation of  $\beta$ -tricalcium phosphate. *Biomaterials* 2003; 24: 4123-31.
- 13) Bigi A, Bracci B, Panzavolta S. Effect of added gelatin on the properties of calcium phosphate cement. *Biomaterials* 2004; 25: 2893-9.
- 14) Li DX, Fan HS, Zhu XD, Tan YF, Xiao WQ, Lu J, et al. Controllable release of salmon-calcitonin in injectable calcium phosphate cement modified by chitosan oligosaccharide and collagen polypeptide. *Journal of Materials Science: Materials in Medicine* 2007; 18: 2225-31.
- 15) Frayssinet P, Roudier M, Lerch A, Ceolin JL, Depre's E, Rouquet N. Tissue reaction against a self-setting calcium phosphate cement set in bone or outside the organism. *Journal of Materials Science: Materials in Medicine* 2000; 11: 811-5.
- 16) Kiyasu K, Takemasa R, Ikeuchi M, Tani T. Differential blood contamination levels and powder-liquid ratios can affect the compressive strength of calcium phosphate cement (CPC): a study using a transpedicular vertebroplasty model. *European Spine Journal* 2013; 22: 1643-9.
- 17) Kon M, Miyamoto Y, Asaoka K, Ishikawa K, Lee H-H. Development of calcium phosphate cement for rapid crystallization to apatite. *Dental materials journal* 1998; 17: 223-32.
- 18) Kanda Y. Investigation of the freely available easy-to-use software 'EZR' for medical statistics. *Bone marrow transplantation* 2013; 48: 452-8.

## Figure and Table captions

- Table 1 Concentration of mixing liquids<sup>10, 17</sup>.
- Table 2 Porosity of  $\beta$ -TCP specimens, 1 week after mixing, according to the P/L ratio.
- Figure 1 Effect of P/L ratio and time after mixing on injectability of  $\beta$ -TCP cement paste. The data for cement (P/L=2.0) are shown in the previous study<sup>10</sup>.
- Figure 2 Initial compressive strength of  $\beta$ -TCP cements. The same letter indicates not significant differences among time after mixing within the same P/L ratio. The same number indicates not significant differences among P/L ratio within the same time after mixing ( $P < 0.05$ ). Data of  $c\beta$ -TCP cement 1 h and 2 h after mixing were excluded from statistical analysis, because the number of specimen was less than 3.
- Figure 3 Initial diametral tensile strength of  $\beta$ -TCP cements. The same letter indicates not significant differences among time after mixing within the same P/L ratio. The same number indicates not significant differences among P/L ratio within the same time after mixing ( $P < 0.05$ ). Data of  $c\beta$ -TCP cement 1 h and 2 h after mixing were excluded from statistical analysis, because the number of specimen was less than 3.
- Figure 4 Compressive strength of  $\beta$ -TCP cement specimens. The same letter indicates not significant differences among storage time within the same P/L ratio. The same number indicates not significant differences among P/L ratio within the same storage time ( $P < 0.01$ ).
- Figure 5 Diametral tensile strength of  $\beta$ -TCP specimens. The same letter indicates not significant differences among storage time within the same P/L ratio. The same number indicates not significant differences among P/L ratio within the same storage time ( $P < 0.01$ ).
- Figure 6 SEM images of fracture surface of diametral tensile strength specimen of  $\beta$ -TCP, 2 weeks after mixing. White arrow indicates porosity and black arrows indicates plate-like crystals.

Figure 7 Specimens implanted in the backs rats for 2 weeks. Those implanted on the left were  $c\beta$ -TCP cement and those implanted on the right were  $m\beta$ -TCP cement.

Figure 8 Compressive strength of  $\beta$ -TCP specimens set in SBF and set in rats.

Figure 9 X-ray diffraction patterns of  $c\beta$ -TCP and  $m\beta$ -TCP specimens set in air, set in SBF, and set *in vivo*. Zirconia peaks originated from contamination from zirconia ball and jar<sup>10</sup>.

Figure 10 Dependence of compressive strength, diametral tensile strength, and porosity of  $\beta$ -TCP specimens 1 week after mixing.

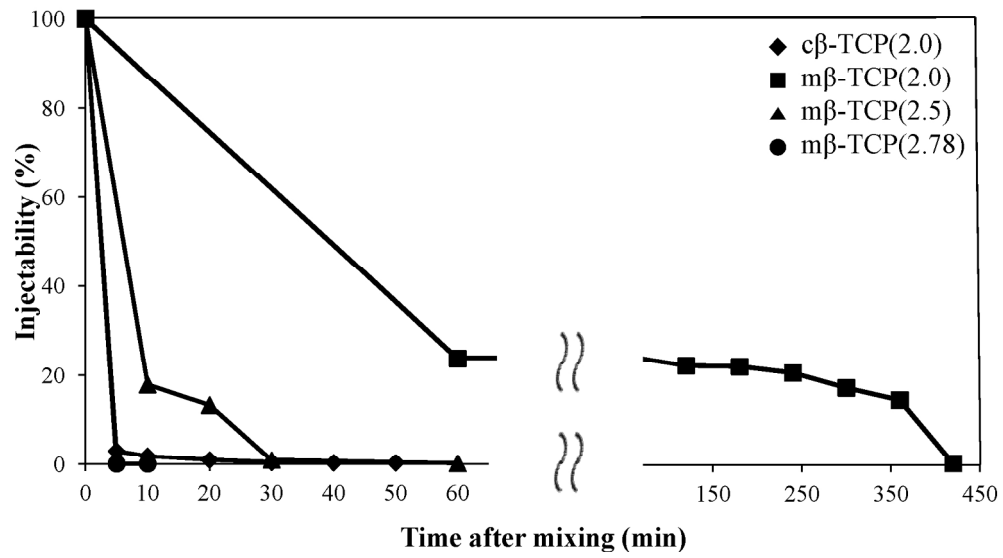
Liquid	P/L (2.0)	P/L (2.5)	P/L (2.78)
First : CaCl <sub>2</sub> solution	1.0 mol/l	1.25 mol/l	1.39 mol/l
Second : NaH <sub>2</sub> PO <sub>4</sub> solution	0.6 mol/l	0.75 mol/l	0.83 mol/l

\* Ca/P ratio of whole mixing liquid=1.67

For Peer Review

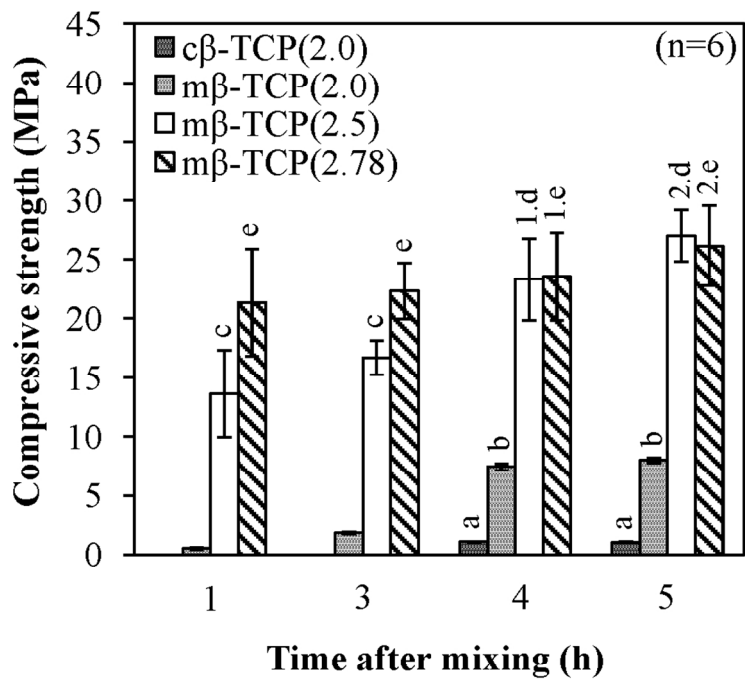
		Porosity (%)
c $\beta$ -TCP	P/L (2.0)	53.2 $\pm$ 0.74
	P/L (2.0)	41.9 $\pm$ 1.97
m $\beta$ -TCP	P/L (2.5)	38.4 $\pm$ 0.89
	P/L (2.78)	47.4 $\pm$ 1.03

For Peer Review

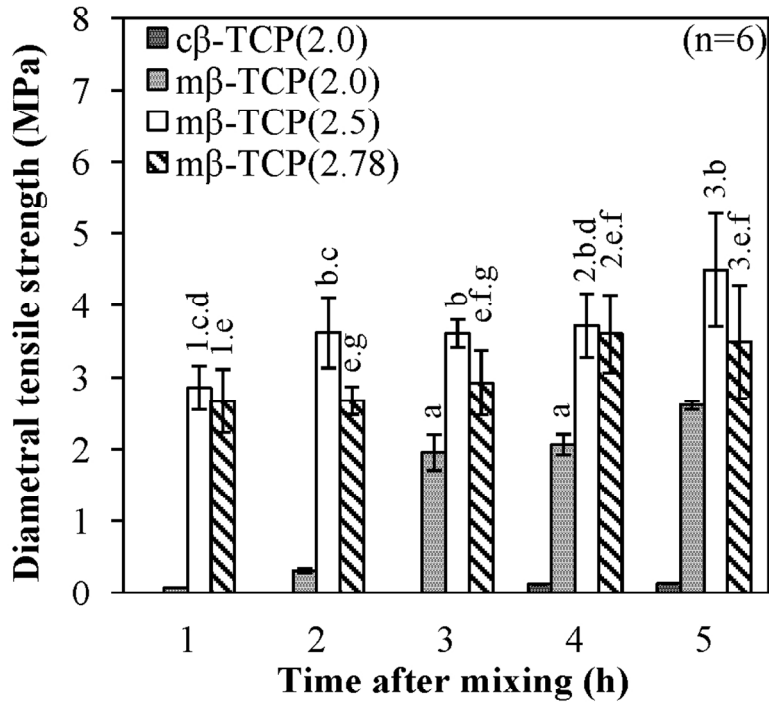


177x100mm (300 x 300 DPI)

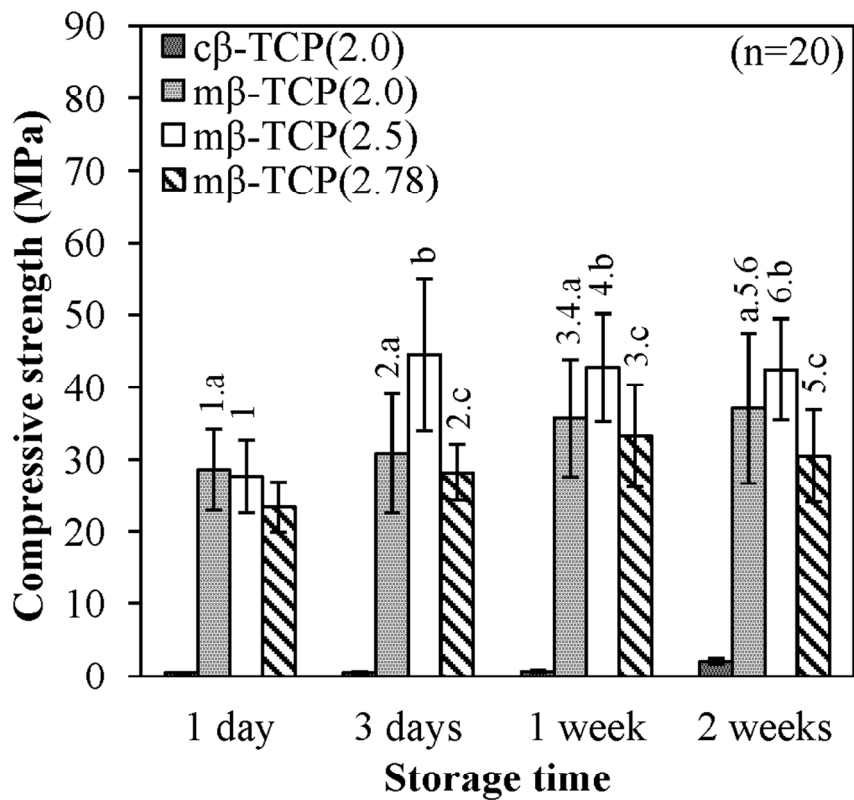
Peer Review



114x99mm (300 x 300 DPI)

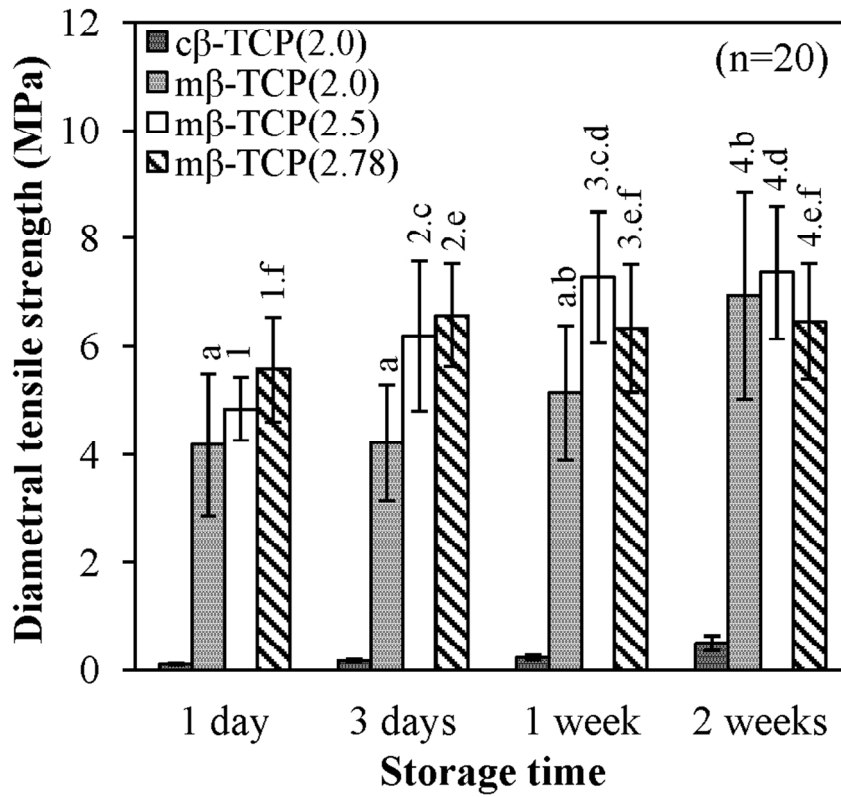


110x95mm (300 x 300 DPI)



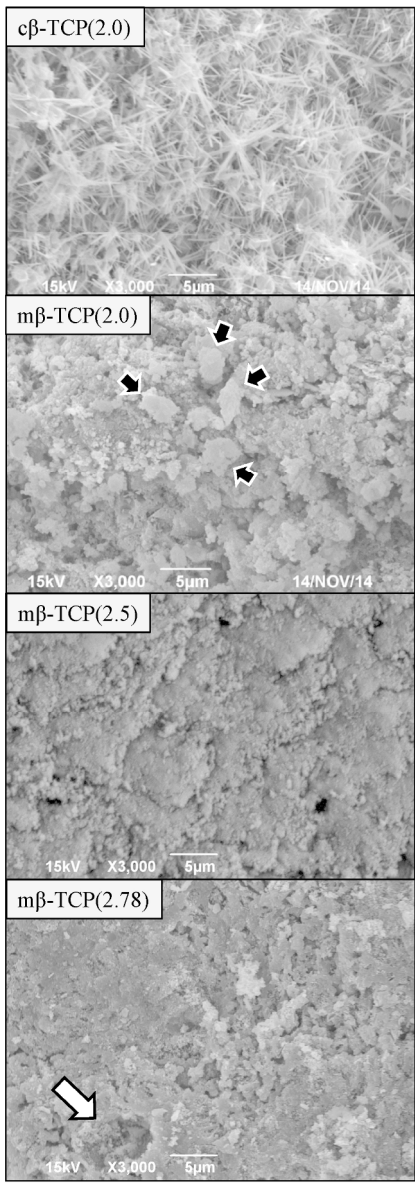
101x97mm (300 x 300 DPI)





101x93mm (300 x 300 DPI)



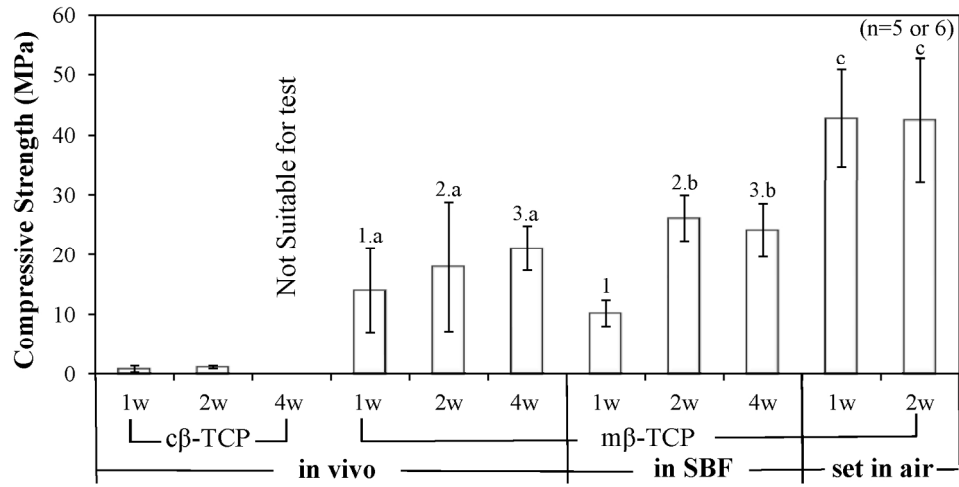


96x265mm (300 x 300 DPI)



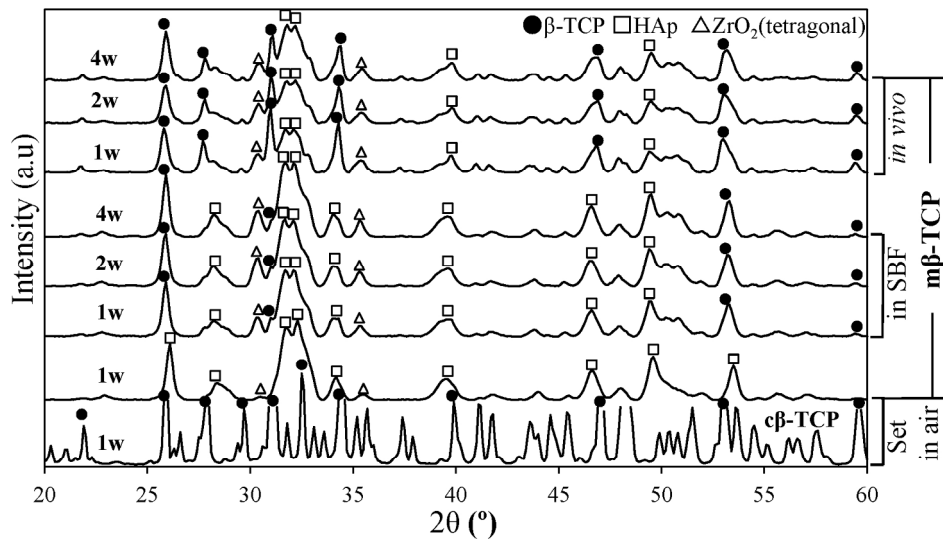
94x44mm (300 x 300 DPI)

Peer Review

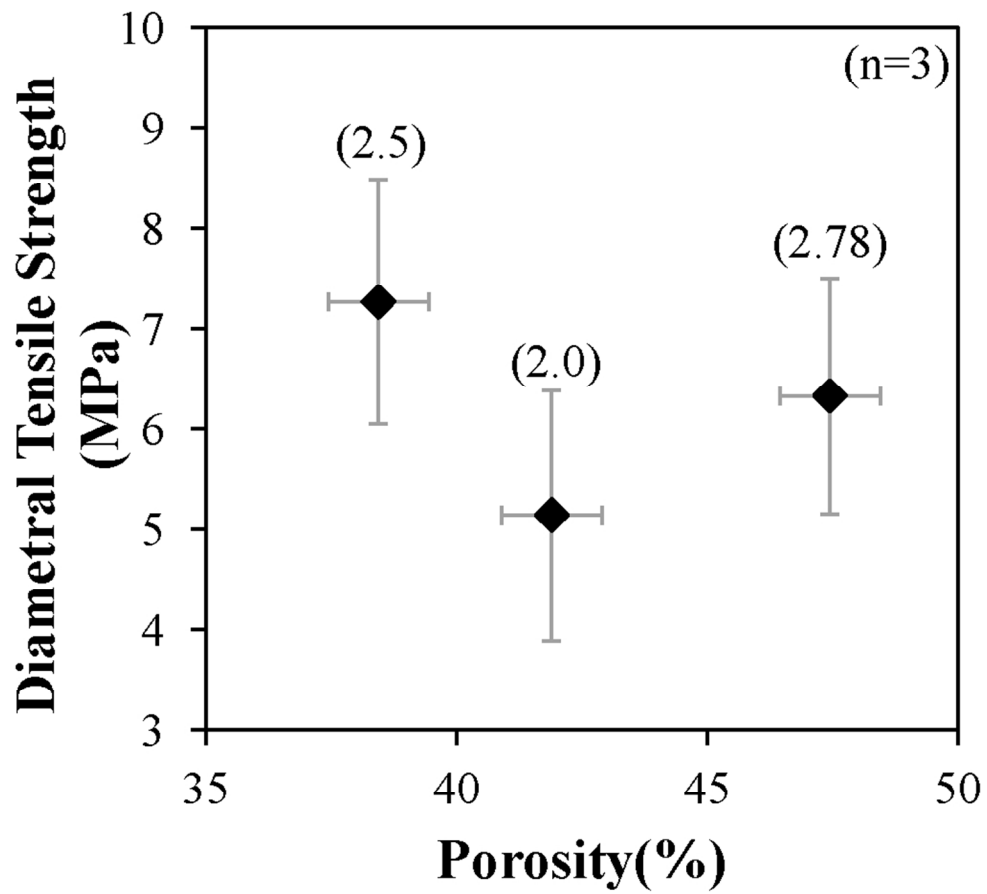


181x100mm (300 x 300 DPI)

er Review



185x106mm (300 x 300 DPI)



88x80mm (300 x 300 DPI)

